Accelerated Publications

Crystal Structure of the Complex between Actin and Human Vitamin D-Binding Protein at 2.5 Å Resolution[†,‡]

James F. Head,[*,§] Narasimha Swamy,[||,⊥] and Rahul Ray[*,||]

Department of Physiology and Biophysics and Bioorganic Chemistry and Structural Biology, Section in Endocrinology, Diabetes and Metabolism, Department of Medicine, Boston University School of Medicine, Boston, Massachusetts 02118

Received May 1, 2002; Revised Manuscript Received May 31, 2002

ABSTRACT: A high-affinity complex formed between G-actin and plasma vitamin D-binding protein (DBP) is believed to form part of a scavenging system in the plasma for removing actin released from damaged cells. In the study presented here, we describe the crystal structure of the complex between actin and human vitamin D-binding protein at 2.5 Å resolution. The complex contains one molecule of each protein bound together by extensive ionic, polar, and hydrophobic interactions. It includes an ATP and a calcium ion bound to actin, but no evidence of vitamin D metabolites bound to the DBP. Both actin and DBP are multidomain molecules, two major domains in actin and three in DBP. All of these domains contribute to the interaction between the molecules. DBP enfolds the end of the actin molecule, principally in actin subdomain 3 but with additional interactions in actin subdomain 1. This orientation is similar to the binding of profilin to actin, as predicted from previous studies. The more extensive interactions of DBP give an affinity for actin some 3 orders of magnitude higher than that for profilin. The larger "footprint" of DBP on actin also leads to an overlap with the actin-binding site of gelsolin domain I.

Vitamin D-binding protein (DBP), also known as a group specific component (Gc), is a polymorphic serum glycoprotein with multiple functions that include vitamin D sterol transport and prevention of arterial congestion in the events of cell injury and lysis by binding actin released into plasma (*1*, *2*). In addition, DBP binds saturated and unsaturated fatty acids with moderate affinity ($K_a \approx 10^5-10^6$ M^{-1}) (*3*) and chemotactic agents (*4*). DBP is also detected on the surface of lymphocytes, neutrophils, and monocytes from blood (*5*−*8*). The physiological implications of these cell-associative properties are currently uncertain.

DBP binds vitamin D_3 and all its major metabolites with high affinity ($K_a \approx 10^7-10^{10}$ M^{-1}). In plasma, DBP binds vitamin D_3 and transports this secosteroid to the liver to form 25-hydroxyvitamin D_3 (25-OH-D_3); the latter in turn is transported (by DBP) to kidney to form 1α,25-dihydroxyvitamin D_3 [1,25$(OH)_2D_3$]. Finally, 1,25$(OH)_2D_3$, the active form of vitamin D hormone, is delivered to target tissues by DBP (*9*). Thus, biological functions of 1,25$(OH)_2D_3$, e.g., calcium and phosphorus homeostasis, immune modulation, regulation of growth, and maturity of normal and malignant cells, are intimately dependent on DBP.

DBP plays an integral role in a circulating actin-scavenger system in plasma that removes actin released into the circulation following cell damage. In this system, it is believed that plasma gelsolin severs filaments of free actin (F-actin), DBP binds monomeric actin (G-actin) with high affinity [$K_a \approx 10^8$ M^{-1} (*10*)], and the DBP−actin complex is rapidly cleared from the circulation (*11*), preventing the harmful effects of polymeric actin clogging arteries (*12*−*14*). There is significant evidence for this clearance process in a variety of disease states (*14*, *15*). The DBP−actin complex is found in the serum of humans and animals that have sustained injuries and/or inflammation, e.g., trophoblastic emboli, severe actute hepatitis, acute lung injury, etc. (*12*).

DBP is a sparsely glycosylated protein (up to 5% glycosylated) with two major phenotypes (Gc1 and Gc2). Yamamoto et al. demonstrated that inflammation-primed B- and T-lymphocytes produce glycosidases to sequentially cleave sugar units from glycosylated DBP (*16*−*18*). The resulting "DBP-*maf*" (macrophage activating factor) acts as a potent activator of macrophages and osteoclasts (*19*−*21*), and has been shown to have potent antitumor activity on Ehrlich Ascites tumor-bearing mice (*22*).

[†] This work was supported by NIH Grant R01 44337 (to R.R.) from the National Institute of Diabetes and Digestive and Kidney Diseases.

[‡] The atomic coordinates for the actin−DBP complex have been deposited in the Protein Data Bank (entry 1LOT).

* To whom correspondence should be addressed. J.F.H.: Department of Physiology and Biophysics, 750 Albany St., Boston, MA 02118; phone, (617) 638-4396; fax, (617) 638-4723; e-mail, head@bu.edu. R.R.: Bioorganic Chemistry and Structural Biology, Section in Endocrinology, Diabetes and Metabolism, Department of Medicine, 750 Albany St., Boston, MA 02118; phone, (617) 638-8199; fax, (617) 638-8194; e-mail, bapi@bu.edu.

[§] Department of Physiology and Biophysics.

[||] Department of Medicine.

[⊥] Current address: Department of Pediatrics, Women and Infant's Hospital, Providence, RI 02905.

10.1021/bi026054y CCC: $22.00
Published on Web 06/26/2002

DBP, a member of the albumin gene family, has a triple-domain modular structure characteristic of the other members of this family (*23*). While DBP serves to transport vitamin D metabolites in the plasma, it can, like albumin, bind fatty acids, but unlike albumin, it also binds G-actin.

Several biochemical studies involving affinity and/or photoaffinity labeling, mutation and/or truncation, and ligand binding suggested that vitamin D sterol binding by DBP is restricted to N-terminal domain 1 of the protein (*24*−*28*). A recent determination of the crystal structure of the DBP−25-OH-D_3 complex confirmed the results of these biochemical studies (*29*).

The structure−function relationship in the DBP−actin interaction has, to date, been unclear. Haddad et al. showed that a segment of DBP (residues 350−403), spanning parts of domains 2 and 3, binds actin, and suggested that actin binding might be independent of vitamin D sterol binding (*24*). However, the effect of actin binding on the transportation of vitamin D metabolites or on macrophage and/or osteoclast activation is largely undetermined.

In the study presented here, we have determined the crystal structure of the DBP−actin complex to provide a detailed structural basis for understanding the interaction between the components and how the formation of the complex may affect other aspects of DBP function, including vitamin D transport and DBP-*maf*-related activities.

EXPERIMENTAL PROCEDURES

Preparation of the DBP−Actin Complex. F-Actin was extracted from rabbit muscle acetone powder (100 mg) in 4 mL of a buffer containing 5 mM Tris-HCl and 2 mM NaN_3 (pH 7.4) by stirring the mixture at 0 °C for 20 min followed by filtration. The filtrate (1 mL) was mixed and incubated for 20 h at 4 °C with human DBP (0.5 mg, Sigma Chemical Co., St. Louis, MO) in a final volume of 5 mL containing 10 mM Tris-HCl, 2 mM NaN_3, 1 mM EDTA, 2 mM $CaCl_2$, and 5 mM ATP (pH 7.6). After this period, the buffer was adjusted to include additional 0.5 mM $MgCl_2$ and 10 mM NaCl, and the resulting solution was stored at 4 °C for an additional 20 h. Following this incubation, the solution was centrifuged at 145000*g* for 2 h at 4 °C to remove the remaining F-actin, and the supernatant, containing the highly enriched DBP−actin complex, was concentrated using a Millipore spin filter concentrator (Millipore Co., Bedford, MA).

Crystallization. The protein complex at 12 mg/mL in 5 mM Tris-HCl, 2 mM sodium azide, 1 mM EDTA, 2 mM $CaCl_2$, and 5 mM ATP (pH 7.6) was mixed in an equal volume with the crystallization buffer, 0.1 M calcium acetate, 0.05 M cacodylate (pH 6.5), 9% PEG 8000, and 10% glycerol in 5 μL drops. Crystals were grown in hanging drops equilibrated by vapor diffusion with the crystallization buffer.

Data Collection and Structure Refinement. Data were collected at the Brookhaven National Synchrotron Light Source, beamline X8C, and indexed, integrated, and scaled using DENZO/Scalepack (*30*). Crystals were flash-frozen in crystallization medium under a stream of nitrogen at 100 K, and data were collected at this temperature. The crystals diffracted to 2.5 Å in space group $P2_12_12_1$ with one molecule of the complex per asymmetric unit and with the following cell dimensions: $a = 80.2$ Å, $b = 87.3$ Å, and $c = 159.6$ Å.

Table 1: Data Collection and Refinement Statistics

data collection	
space group	$P2_12_12_1$
unit cell dimensions *a*, *b*, and *c* (Å)	80.17, 87.34, 159.58
maximum resolution (Å)	2.5
total no. reflections measured (no. of unique reflections)	473796 (39585)
overall completeness (%) (highest-resolution shell)	99.3 (96.7)
overall R_{merge}[a] (highest-resolution shell)	0.060 (0.276)
refinement	
resolution range (Å)	50−2.5
R_{cryst}[b]	0.223
R_{free} (8% test set)	0.275
no. of protein atoms [mean *B*-factor for DBP/actin (Å^2)]	6234 (55.9/47.6)
no. of Ca^{2+} ions (*B*-factor)	1 (40.7)
no. of ATPs (group *B*-factor)	1 (50.3)
no. of water molecules (mean *B*-factor)	88 (42.4)
rmsd for angles (deg)	0.007
rmsd for bonds (Å)	1.3
no. of residues	796
Ramachandran plot, most favored (%)	90.0
Ramachandran plot, disallowed (%)	0.0

[a] $R_{merge} = \sum|I_I - \langle I\rangle|/\sum I_I \times 100$, where I_I is the intensity of an individual reflection and $\langle I\rangle$ is the mean intensity of that reflection. [b] $R_{cryst} = \sum||F_p| - |F_{calc}||/\sum|F_p| \times 100$, where $|F_{calc}|$ is the calculated structure factor.

Data collection statistics are shown in Table 1. Crystal growth and crystal parameters have been reported elsewhere (*31*).

The data were phased by molecular replacement using the program AmoRe (*32*). A starting model of rabbit G-actin was derived from the structure of the actin−DNAse I structure [Protein Data Bank (PDB) entry 1ATN] (*33*) and that of DBP from subunit "A" of the structure of DBP (PDB entry 1J78) (*29*).

The structure was refined from the molecular replacement solution using CNS (*34*) with cycles of refinement and rebuilding using the molecular graphics program O (*35*). Models, parameter and other files for building and refining *N*-methylhistidine, and the ligand ATP were obtained from the HICUP database (*36*). Refinement was performed, and solvent molecules were added only as consistent with a reduction in R_{free}. Refinement statistics are presented in Table 1.

RESULTS

Interactions of Actin with DBP. Actin, ubiquitous in cells, is able to interact with a large number of different proteins, some involved in contractile regulation, some in filament bundling and attachment, and others in filamentogenesis, severing, and capping. Crystal structures have previously been determined for G-actin complexes with DNAse I (*33*), gelsolin domain I (*37*), and profilin (*38*). These proteins each interact differently with the actin molecule. In this communication, we describe the three-dimensional structure of the DBP−actin complex, which provides insights into the structural basis for the differential binding effects of actin with DBP, gelsolin, and profilin. Another report on the growth of crystals of the DBP−actin complex was published recently (*39*), although the crystals belonged to a space group different from the space group of those described in this study.

As shown in Figure 1, DBP binds to actin by enfolding the end of the oblate actin molecule, primarily at actin

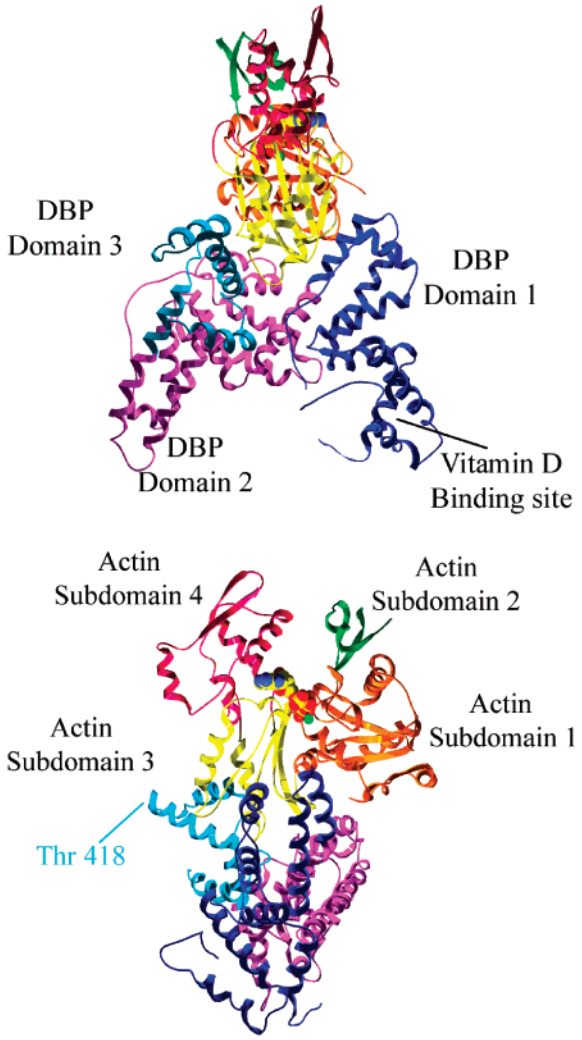

FIGURE 1: Ribbon representations of two orthogonal views of the DBP−actin complex: orange, actin subdomain 1; green, actin subdomain 2; yellow, actin subdomain 3; red, actin subdomain 4; blue, DBP domain 1; magenta, DBP domain 2; and cyan, DBP domain 3 (color-coded as in ref *29*). ATP and Ca^{2+} (green) are shown as space-filling representations.

subdomain 3 but extending to subdomain 1. The groove in DBP that accommodates the actin is flanked on one side by part of DBP domain 1 and on the other by part of domain 3. The bottom of the groove is contributed by part of domain 2. The interface between the molecules is extensive, involving many residues in ionic and polar interactions (see Table 2) as well as some hydrophobic interactions, leading to the burial of 3680 $Å^2$ of the combined surfaces. This buried surface is approximately 50% greater than that in the actin−profilin complex (*38*).

The actin molecule includes a bound ATP and an associated calcium ion. Although the structure is grown in the presence of high calcium concentrations, we see no evidence of other bound calcium ions in this structure. DBP contains no apparent vitamin D. DBP residues 91−111 and actin residues 1, 2, 40−50, 374, and 375 appear to be disordered in this structure and are absent from the model. There is no apparent electron density corresponding to the bound sugar at the glycosylation site, Thr 418, probably because of high mobility in the absence of stabilizing contacts at this exposed surface site.

Table 2: Hydrogen Bonds between DBP and Actin

DBP residue (atom)	actin residue (atom)	distance (Å)
Y120 (O)	K291 (NZ)	2.7
P123 (O)	R147 (NH2)	2.5
N125 (ND2)	S145 (O)	3.1
N125 (ND2)	G146 (O)	3.0
N125 (OD1)	R147 (NE)	2.8
E127 (OE1)	K328 (NZ)	2.8
Y151 (OH)	K291 (NZ)	2.9
R187 (NE)	G146 (O)	2.9
K191 (NZ)	E167 (O)	2.8
S194 (OG)	E167 (OE2)	3.1
R202 (NH2)	D288 (OD2)	2.9
Q285 (OE1)	K113 (NZ)	3.1
N397 (O)	K284 (NZ)	3.1
F399 (N)	N280 (OD1)	3.3
T400 (OG1)	N280 (ND2)	2.9
S434 (O)	R290 (NH2)	3.1
N440 (ND1)	D286 (OD2)	3.1

While the large contact area leaves no ambiguity about which is the physiologically significant interaction between actin and DBP in this structure, there are other intermolecular contacts between different actin and DBP molecules in the crystal. These contacts involve only a few residues in each case, and are typical of crystal packing contacts. While the contacts are small, it is possible that they may be of some significance to the structure of the complex observed in the crystal (see below). The domains and subdomains of both actin and DBP are separated by linker regions that appear to provide significant flexibility. Even small peripheral interactions may therefore have some influence on the disposition of the domains.

Structural Changes in Actin and DBP in the Complex. The interpretation of the changes in the actin and DBP molecules in the complex is predicated on the models chosen as the unbound form of each protein. In this work, the molecule of DBP in the complex can be compared to each of the two molecules, A and B, in the asymmetric unit of the published crystal structure of DBP alone (PDB entry 1J78) (*29*). Molecule A, like DBP in the present structure, has no bound vitamin D, whereas molecule B contains 25-hydroxyvitamin D_3 (25-OH-D_3). For comparison with actin, we have chosen the actin molecule contained in the actin−DNAse I structure (*33*). Although a crystal structure of actin alone is available (PDB entry 1J6Z) (*40*), this molecule was considered to be unsuitable for comparative purposes since it contains ADP rather than ATP, which has structural consequences itself. The present structure, and that of the actin−DNAse complex, both contain ATP. Since the site of DNAse binding to G-actin is remote from the site of DBP binding, any DNAse-induced changes in the actin structure in the DNAse complex are unlikely to compromise the interpretation of local changes in actin induced by DBP.

In actin-bound DBP, the flanking walls of the actin-binding groove are displaced somewhat toward one another compared to those in molecule "A" of DBP alone, resulting in a "gripping" of the actin. The "mouth" of the groove closes by 3.6 Å (measured from T124 Cα to T400 Cα). This closure is accompanied by an apparently compensatory opening of "lobes" at the other end of the molecule, as if by a lever effect around the center of the molecule (Figure 2). This picture supports an earlier observation which indicated that the conformation of DBP is altered by actin binding, as

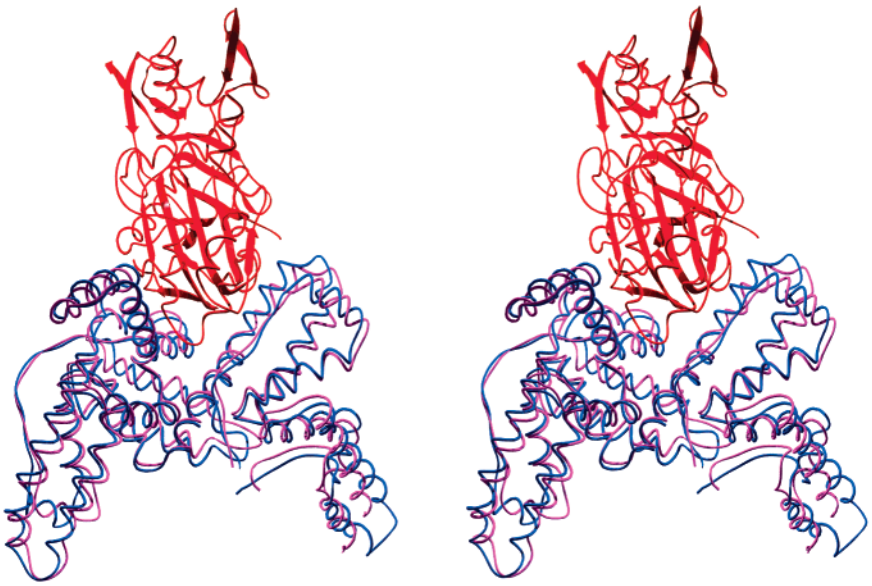

FIGURE 2: Stereoview of the superimposition of DBP alone on the DBP−actin structure: red, actin; blue, DBP bound to actin; and magenta, DBP alone (molecule A of PDB entry 1J78) (*29*). The orientation is as in the top panel of Figure 1.

assessed by fluorescence quenching of 2-*p*-toluinidylnaphthalene-6-sulfonate, a hydrophobic probe (*41*).

Some of these gross changes in DBP can be ascribed to rigid-body rotations of the domains. The rms deviations of Cαs for a least-squares superposition of whole bound and unbound DBP (A) molecules are as follows: 2.08 Å for all residues, 2.57 Å for domain 1, 1.91 Å for domain 2, and 1.06 Å for domain 3. A least-squares superposition of domain 1 alone, equivalent to allowing a rigid body movement of this domain, gives a much closer rmsd of 1.36 Å (1.56 Å for domain 2 alone), and domain 3 alone aligns very closely with an rmsd of 0.64 Å. Some additional flexibility arises within extended structures in domain 1 between helices 6 and 7, and in domain 2 between helices 6 and 8, that accommodates further movement of the "subdomains" on either side of these regions. These helix designations are based on the equivalent assignments in serum albumin, as used in descriptions of the structure of DBP (*29*).

Comparison of the actin-bound DBP with the 25-OH-D_3-containing "B" molecule of DBP alone shows a less pronounced difference, superimposing better with an overall rms deviation of 1.7 Å. One of the major differences between these structures is in the N-terminal subdomain, residues 5−91, which includes the vitamin D binding site. In the overall superposition, this region has an rms deviation of 2.3 Å. Rotation as a rigid body superimposes this N-terminal subdomain closely, with an rms deviation of 1.0 Å. The relative rotation induced by the binding of 25-OH-D_3 is apparently accommodated by flexibility in the loop of residues 90−110, which is partly disordered in both structures.

Previous biochemical studies have shown that DBP bound to 25-OH-D_3 or 1,25$(OH)_2D_3$ produced a complex with actin that appears to be indistinguishable from the DBP−actin complex without the vitamin D ligands (*42*). We have also used 25-OH-D_3 affinity chromatography to purify the DBP−actin complex from a crude mixture of rabbit muscle F-actin and human plasma, and to show that this complex bound 25-OH-D_3 in a manner qualitatively similar to that of DBP alone (*31*). Collectively, these results show that DBP can bind actin and vitamin D sterols at the same time. However, we find that DBP−actin crystals grown without vitamin D become cracked and disordered by addition of 25-OH-D_3 to the mother liquor, indicating a structural interdependence between actin and 25-OH-D_3 binding. We believe this crystal disruption may be explained by observed structural difference between vitamin D-bound and actin-bound DBP. A loop region near the vitamin D-binding site forms a crystal contact in the DBP−actin complex, at Gly 62, that constrains the loop. The binding of vitamin D induces a rotation of the N-terminal subdomain that may then disrupt this contact, leading to a loss of crystal order. The physiological significance of this change is unclear, and the relative affinity of DBP for vitamin D in the presence and absence of actin remains to be determined.

Superposition of the actin of the DBP complex with that of the DNAse complex shows close similarity, with an rms deviation of 1.04 Å for all observed residues. Residues 40−49 of actin are not ordered in the DBP−actin complex but, as part of the DNAse binding site, are well-ordered in the actin−DNAse complex. Other regions of significant deviation between these actin structures are at the N-terminus (residues 3−6) and residues 193−197 in subdomain 4. Omitting these regions reduces the rms deviation of the overall superimposition to 0.74 Å. The relative deformation in these two regions appears to result from a crystal packing contact between the extended N-terminus of one actin and residue 197 in an adjacent actin molecule in the crystal.

Several actin residues involved in contacts with DBP are the same as those in contact with profilin (K113, D286, D288, R290, H371, and R372), although the binding surface of DBP bears little resemblance to that of profilin (Figure 3). In DBP, this surface consists mostly of helical secondary structure elements, while that of profilin is largely β-sheet. A common binding site for DBP and profilin on actin had previously been predicted, on the basis of differential binding and displacement studies (*43*). However, profilin binds actin weakly ($K_a \approx 2 \times 10^5$ M^{-1}) (*41*, *44*) and is readily displaced by DBP ($K_a \approx 10^8$ M^{-1}) (*41*, *43*).

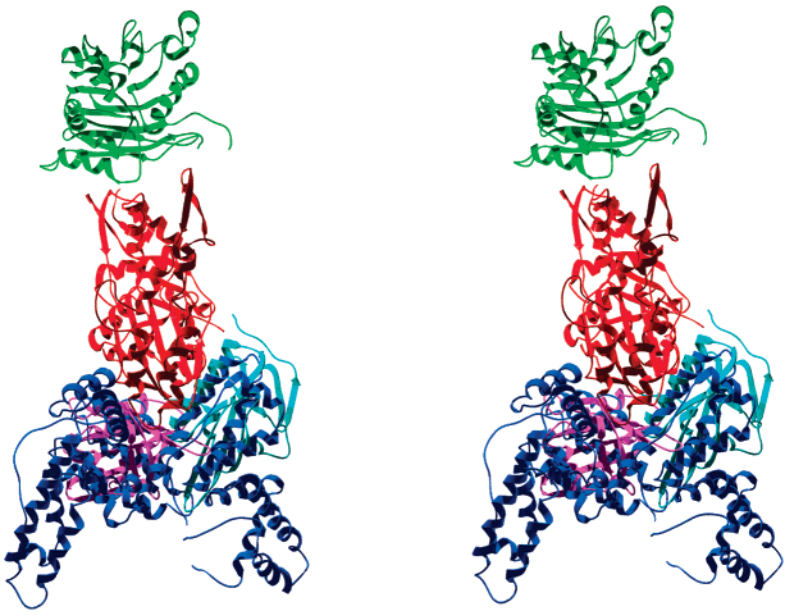

FIGURE 3: Stereoview of the superimposition of actin-binding proteins. Molecules are aligned on the basis of least-squares superimposition of the actin in each structure, although only the actin of the DBP−actin complex is shown. The orientation is as in the top panel of Figure 1: red, actin from the DBP−actin complex; blue, DBP from the DBP−actin complex; cyan, gelsolin domain 1 (PDB entry 1EQY) (*37*); magenta, profilin (PDB entry 2BTF) (*38*); and green, DNAse (PDB entry 1ATN) (*33*).

The interaction site for DBP also includes part of the gelsolin domain I-binding site on actin, supporting the results of biochemical studies that show competition between DBP and gelsolin for G-actin (*45*, *46*). Helix 10 in domain 1 of DBP (residues 180−190) is oriented in a manner similar to that of residues 72−82 of the interacting helix of gelsolin domain 1 (Figure 3). Little other similarity seems to be shared in these helices beyond a common cluster of hydrophobic interactions with the underlying helix of residues 337−349 of actin. In gelsolin, the helix of residues 72−82 has a high hydrophobic amino acid content and is largely removed from solvent when bound to actin, whereas helix 10 of DBP remains partly solvent exposed and is amphipathic. Surrounding secondary structural elements in DBP and gelsolin appear to be unrelated.

Formation of the complex between actin and DBP appears to somewhat stabilize the thermal motion of DBP, reducing the overall average *B*-factor of observed protein atoms from 60.5 Å^2 (as seen in DBP alone, PDB entry 1J78) (*29*) to 55.9 Å^2 (Table 1), but significantly increases that of the actin to 47.6 Å^2 from 36.6 Å^2 (as seen in the actin component of the actin−DNAse complex, PDB entry 1ATN) (*33*).

DISCUSSION

In providing details of the interaction of actin with DBP, the present structure explains the relative characteristics of binding of profilin, gelsolin, and DBP to actin. The relationship with gelsolin in particular is of potential physiological importance since a model has been proposed in which plasma gelsolin acts to depolymerize F-actin released from damaged cells, and DBP binds the G-actin subunits, promoting clearance of the actin (*11*). The partial sharing of a gelsolin-binding site on actin provides a basis for a mechanism in which DBP displaces gelsolin from depolymerized actin (*46*).

The vitamin D-binding site at the N-terminus of DBP, as predicted in various functional studies (*24*−*28*, *47*) and shown by the crystal structure (*29*), is in domain 1, remote from the actin-binding region. However, the DBP−actin structure shows that part of DBP domain 1 interacts with actin (Figure 1). Therefore, conformational changes induced by the binding of actin might be propagated through the length of the structure, and the binding of actin and vitamin D sterols to DBP may yet prove to have an influence on one another.

The function of DBP as a macrophage and osteoclast activator involves enzymatic deglycosylation of the carbohydrate structure at threonine 418 (*16*, *17*). It is of note that this residue is located at the exposed end of a loop extending from the molecule in the structure of DBP alone (*29*) and also in the present structure of the DBP−actin complex (Figure 1). This location suggests that interactions of glycosidases and of potential cell surface receptors at this site are unimpeded in DBP. The binding of 25-OH-D_3 to DBP alone does not affect osteoclast activation (*21*). However, whether the adjacent actin molecule in the DBP−actin complex alters this function remains to be determined.

NOTE ADDED IN PROOF

Since this paper has been in press, an independent solution of the crystal structure of the actin−DBP complex has been published (*48*).

REFERENCES

1. Cooke, N. E., and Haddad, J. G. (1995) *Endocr. Rev. 4*, 125−128.
2. Haddad, J. G. (1995*) J. Steroid Biochem. Mol. Biol. 53*, 579−582.
3. Calvo, M., and Ena, J. M. (1989) *Biochem. Int. 19*, 1−7.
4. Piquette, C. A., Robinson-Hill, R., and Webster, R. O. (1994) *J. Leukocyte Biol. 55*, 349−354.
5. Kew, R. R., Sibug, M. A., Liuzzo, J. P., and Webster, R. O. (1993) *Blood 82*, 274−283.
6. Petrini, M. D., Emerson, D. L., and Galbraith, R. M. (!983) *Nature 306*, 73−74.
7. Petrini, M. D., Galbraith, R. M., Emerson, D. L., Nel, A. E., and Arnaud, P. (1985) *J. Biol. Chem. 260*, 1804−1810.

8. Guoth, M., Murgla, A., Smith, R., Prystwsky, M., Cooke, N., and Haddad, J. G. (1990) *Endocrinology 127*, 2313−2321.
9. Ray, R. (1998) in *Vitamin D: Physiology, Molecular Biology and Clinical Applications* (Holick, M. F., Ed.) pp 147−162, Humana Press, Totowa, NJ.
10. Haddad, J. G. (1982) *Arch. Biochem. Biophys. 213*, 538−544.
11. Lind, S. E., Smith, D. B., Janmey, P. A., and Stossel, T. P. (1986) *J. Clin. Invest. 78*, 736−742.
12. Lee, W. M., and Galbraith, R. M. (1992) *N. Engl. J. Med. 326*, 1335−1341.
13. Goldschmidt-Clermont, P. J., Williams, M. H., and Galbraith, R. M. (1987) *Biochem. Biophys. Res. Commun. 146*, 611−617.
14. Harper, K. D., McLeod, J. F., Kowalski, M. A., and Haddad, J. G. (1987) *J. Clin. Invest. 79*, 1365−1370.
15. Dahl, B., Schiodt, F. V., Gehrchen, P. M., Ramlau, J., Kaier, T., and Ott, P. (2001) *Inflammation Res. 50*, 39−43.
16. Yamamoto, N., and Homma, S. (1991) *Proc. Natl. Acad. Sci. U.S.A. 88*, 8539−8543.
17. Yamamoto, N., Homma, S., and Millman, I. (1991) *J. Immunol. 147*, 273−280.
18. Yamamoto, N., and Kumashiro, R. (1993) *J. Immunol. 151*, 2794−2802.
19. Yamamoto, N., Lindsay, D. D., Naraparaju, V. R., Ireland, R. A., and Popoff, S. N. (1994) *J. Immunol. 152*, 5100−5107.
20. Schneider, G. B., Benis, K. A., Flay, N. W., Ireland, R. A., and Popoff, S. N. (1995) *Bone 16*, 657−662.
21. Swamy, N., Ghosh, S., Schneider, G. B., and Ray, R. (2001) *J. Cell. Biochem. 81*, 535−546.
22. Yamammoto, N., and Naraparaju, V. R. (1997) *Cancer Res. 57*, 2187−2192.
23. Cooke, N. E., and David, E. V. (1985) *J. Clin. Invest. 76*, 2420−2424.
24. Haddad, J. G., Hu, Y. Z., Kowalski, M. A., Laramore, C., Ray, K., Robzyk, P., and Cooke, N. E. (1992) *Biochemistry 31*, 7174−7181.
25. Ray, R., Bouillon, R., Van Baelen, H. G., and Holick, M. F. (1991) *Biochemistry 30*, 7638−7642.
26. Swamy, N., Dutta, A., and Ray, R. (1997) *Biochemistry 36*, 7432−7436.
27. Swamy, N., Addo, J. K., Uskokovic, M. R., and Ray, R. (2000) *Arch. Biochem. Biophys. 373*, 471−478.
28. Addo, J. K., Swamy, N., and Ray, R. (2002) *Bioorg. Med. Chem. Lett. 12*, 279−281.
29. Verboven, C., Rabijns, A., De Maeyer, M., Van Baelen, H., Bouillon, R., and De Ranter, C. (2002) *Nat. Struct. Biol. 2*, 131−136.
30. Otwinowski, Z. (1993) in *CCP4 Proceedings*, pp 56−62, Daresbury Laboratory, Warrington, U.K.
31. Swamy, N., Head, J. F., Weitz, D., and Ray, R. (2002) *Arch. Biochem. Biophys. 402*, 14−23.
32. Collaborative Computational Project, Number 4 (1994) *Acta Crystallogr. D50*, 760−763.
33. Kabsch, W., Mannherz, H. G., Suck, D., Pai, E. F., and Holmes, K. C. (1990) *Nature 347*, 37−44.
34. Brunger, A. T., Adams, P. D., Clore, G. M., Delano, W. L., Gros, P., Gross-Kunstleve, R. W., Jiang, J.-S., Kuszewski, J., Nilges, M., Pannu, N. S., Read, R. J., Rice, L. M., Simonson, T., and Warren, G. L. (1998) *Acta Crystallogr. D54*, 905−921.
35. Jones, T. A., Zou, J. Y., Cowan, S. W., and Kjeldgaard, M. (1991) *Acta Crystallogr. A47*, 110−119.
36. Kleywegt, G. J., and Jones, T. A. (1998) *Acta Crystallogr. D54*, 1119−1131.
37. McLaughlin, P. J., Gooch, J. T., Mannherz, H. G., and Weeds, A. G. (1993) *Nature 364*, 685−692.
38. Schutt, C. E., Myslik, J. C., Rozycki, M. D., Goonesekere, N. C., and Lindberg, U. (1993) *Nature 365*, 810−816.
39. Bogaerts, I., Verboven, C., Rabijns, A., Waelkens, E., Van Baelen, H., and De Ranter, C. (2001) *Acta Crystallogr. D57*, 740−742.
40. Otterbein, L. R., Graceffa, P., and Dominguez, R. (2001) *Science 293*, 616−618.
41. Goldschmidt-Clermont, P. J., Williams, M. H., and Galbraith, R. M. (1987) *Biochem. Biophys. Res. Commun. 146*, 611−617.
42. McLeod, J. F., Kowalski, M. A., and Haddad, J. G. (1989) *J. Biol. Chem. 264*, 1260−1267.
43. Goldschmidt-Clermont, P. J., Van Alstyne, E. L., Day, J. R., Emerson, D. L., Nel, A. E., Lazarchick, J., and Galbraith, R. M. (1986) *Biochemistry 25*, 6467−6472.
44. Lal, A. A., and Korn, E. D. (1985) *J. Biol. Chem. 260*, 10132−10238.
45. Coue, M., Constans, J., and Olomucki, A. (1986) *Eur. J. Biochem. 160*, 273−277.
46. Ohsawa, M., and Kimura, H. (1989) *Biochim. Biophys. Acta 992*, 195−200.
47. Swamy, N., Brisson, M., and Ray, R. (1995) *J. Biol. Chem. 270*, 2636−2639.
48. Otterbein, L. R., Cosio, C., Graceffa, P., and Dominguez, R. (2002) *Proc. Natl. Acad. Sci. U.S.A. 99*, 8003−8008.

BI026054Y